ASME International
The American Society of Mechanical Engineers
345 East 47th Street
New York, NY 10017

Reprinted From
DSC-Vol. 58, Proceedings of the Dynamic Systems and Control Division
Editor: Kourosh Danai
Book No. G01023 – 1996

A NEW MULTI–FINGER TACTUAL DISPLAY

Hong Z. Tan and William M. Rabinowitz
Massachusetts Institute of Technology
Research Laboratory of Electronics
Sensory Communication Group
50 Vassar Street, Room 36-755
Cambridge, Massachusetts, 02139, USA
Tel. (617) 253-8921
Fax. (617) 258-7003
Email: tan@cbgrle.mit.edu

ABSTRACT

A multi-finger positional display (the TACTUATOR) was developed to study communication through the kinesthetic and vibrotactile aspects of the tactual sensory system of the hand. The display consists of three independent single contact-point actuators interfaced (individually) with the fingerpads of the thumb, the index finger, and the middle finger. Each actuator utilizes a disk-drive head-positioning motor augmented with angular position feedback from a precision rotary variable differential transformer (RVDT). A floating-point DSP system provides real-time positional control using a digital PID controller. Stimuli from threshold to about 50 dB SL can be delivered throughout the frequency range from near DC to above 300 *Hz*, thereby encompassing the perceptual range from gross motion to vibration. Actuator frequency and step responses are well modeled as a second-order linear system. Distortion is low allowing delivery of arbitrary stimulus waveforms, e.g., 25 *mm* low-frequency motion with superimposed high-frequency vibration. System noise and inter-channel crosstalk are also small. As one example of behavioral performance verification, absolute thresholds measured with the stimulator are in general agreement with values in the literature. Overall, the TACTUATOR accurately follows its drive waveforms and is well suited for a variety of multi-finger tactual perceptual studies.

INTRODUCTION

This work was motivated by our interest in using the sense of touch as an alternative communication channel. One application area for this work is sensory substitution for individuals who are hearing-impaired and/or visually-impaired. It also provides a new haptic interface for exploring novel human-computer interactions through the tactual channel.

The potential to receive information tactually is well illustrated by some natural (i.e., non-device related) methods of tactual speech communication. Particularly noteworthy is the so-called Tadoma method that is employed by some individuals who are both deaf and blind. In Tadoma, one places a hand on the face and neck of a talker and monitors a variety of actions associated with speech production. Our previous research has documented the remarkable abilities of experienced Tadoma users (Reed, Rabinowitz, Durlach, Braida, Conway-Fithian, & Schultz, 1985); these individuals can understand everyday speech at very high levels, allowing rich two-way conversation with both familiar and novel talkers. Conversely, attempts to develop artificial tactual speech communication devices have had only limited success, with none achieving performance anywhere near that demonstrated by Tadoma (e.g., Reed, Durlach, Delhorne, Rabinowitz, & Grant, 1989).

One problem with most previous tactual devices concerns the nature of the output display. These displays have generally been composed of multiple stimulators that deliver high-frequency vibration to the cutaneous sensory system. Such "homogeneous" displays have few distinctive perceptual qualities. Furthermore, for practical and/or technical reasons, the displays have rarely engaged the hand, the most sensitive and richly innervated receiving site. In contrast, Tadoma is received by the hand and a talking face is perceptually rich, simultaneously displaying various stimulation qualities that engage both the kinesthetic and cutaneous sensory systems.

Recognition of the need for richer tactual displays is now prevalent. Our group has developed an artificial mechanical face display, built around a model plastic skull (Reed *et al.*, 1985), that has shown promise in conveying information important in Tadoma (Leotta, Rabinowitz, Reed, & Durlach, 1988; Rabinowitz, Henderson, Reed, Delhorne, & Durlach, 1990). As a more general display for studying haptic perception by the hand, the "OMAR" system was recently described by Eberhardt, Bernstein, Barac-Cikoja, Coulter, & Jordan (1994). It was designed to deliver kinesthetic as well as cutaneous stimulation to one or more fingers.

The present research is directed at a display that shares some features with OMAR. Our display, the "TACTUATOR", aims at a

continuous frequency response so that the perception from low-frequency large-amplitude motions to high-frequency small-amplitude vibrations can be studied as a continuum. The TACTUATOR applies independent stimulation to the fingerpads of the thumb, index, and middle fingers. Each fingerpad receives one-degree-of-freedom motion, via single contact-point actuators. The motion trajectory for the thumb is perpendicular to that of the index and middle fingers, thereby maintaining an approximately natural hand configuration (see Fig. 1).

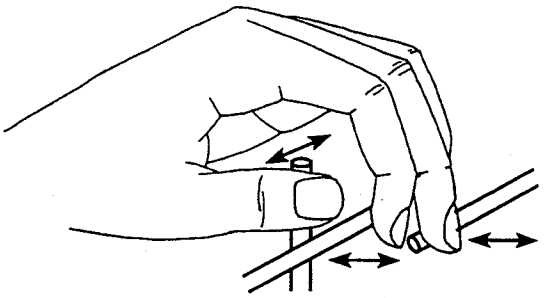

Figure 1. Schematic drawing illustrating finger placement on the TACTUATOR.

The main challenge for the design was to have an actuator that could operate over the required amplitude-frequency range. Specifically, our design goal was to cover the frequency range from near DC to about 300 *Hz* with amplitudes from absolute threshold (the smallest displacement that can be detected) to about 54 dB above threshold, i.e., 54 dB SL[1] (or, equivalently, 500 times the threshold displacement). This range spans the tactual stimulation area that is comfortable (e.g., Verrillo & Gescheider, 1992). The actuator's displacement requirements then follow from normative tactual thresholds. Representative results from Bolanowski, Gescheider, Verrillo, & Checkosky (1988) (see Fig. 2) show thresholds that are constant (at 26 dB relative to 1 *μm* peak, i.e., 40 *μm* peak-to-peak) up to about 3 *Hz*, decreasing at a rate of about −5 dB/octave up to 30 *Hz* and, then, −12 dB/octave up to 300 *Hz*, after which threshold increases.

A closed-loop, position-controlled actuator system has been developed that (essentially) meets the above specifications. We describe the system, document its performance with a variety of physical measurements, and include an example behavioral assessment.

SYSTEM OVERVIEW

The overall system consists of three independent motor assemblies that are interfaced with the thumb, the index finger, and the middle finger, respectively (Fig. 3). An angular position sensor

1. Sensation level (denoted *dB SL*) is defined as the signal level in decibels relative to the detection threshold.

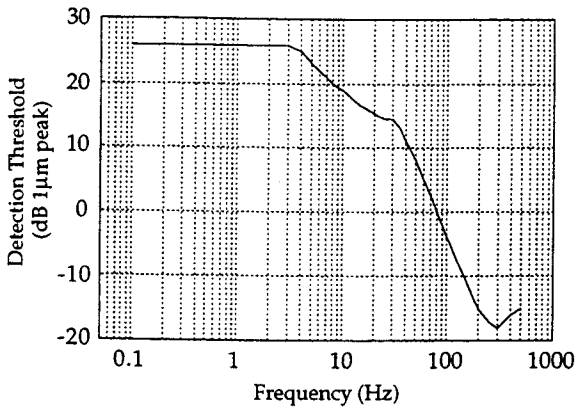

Figure 2. Detection threshold from Bolanowski *et al.* (1988).

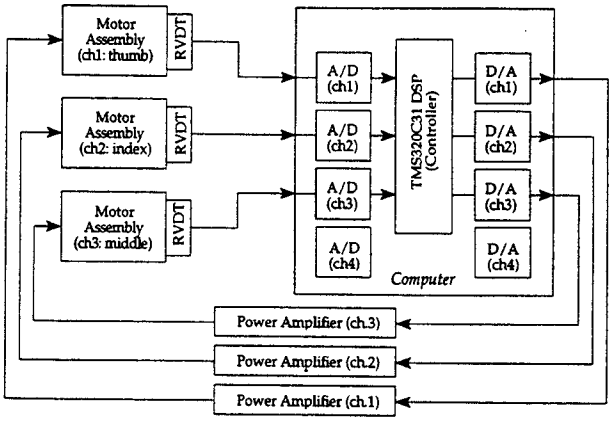

Figure 3. TACTUATOR system diagram.

(RVDT) is attached to the moving part of each of the three motor assemblies. The sensor transforms the angular position of each actuator to a DC voltage, which is then sampled by a corresponding 16-*bit* analog-to-digital converter. Within a TMS320C31-based floating-point DSP environment, each sampled sensor voltage is compared to a reference voltage. A digital command signal is then computed from this error signal using a proportional-integral-differential (PID) controller. This command signal is applied to a corresponding 16-*bit* digital-to-analog converter, amplified, and sent to the actuator. This process completes one cycle of the closed-loop control. Details of important components are discussed below.

Hardware Components

Motor Assembly. The head-positioning motor from a Maxtor hard-disk drive was selected as the actuator because of its high bandwidth and smooth operation at very low frequencies. Fully-

assembled disk drives were stripped of electronic components. The original casing was cut so that only the head-positioning motor and its bearing and supporting structures remained (Fig. 4). Additional hardware was designed around this remaining structure to position it in the desired orientation ("V block"), to provide an interface site for the fingerpad, and to align the angular position sensor with the motor's bearing ("sensor support"). The actuator has two built-in mechanical stops which limit its range of motion to slightly less than 30°. With an armature of length 50 *mm*, the achievable range of motion is 26 *mm* (peak-to-peak).

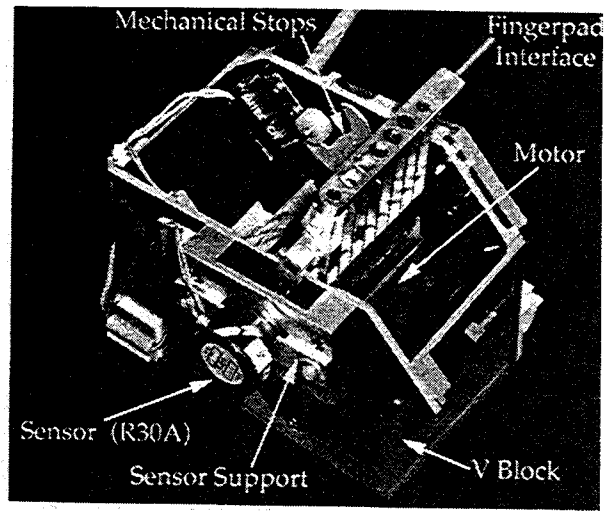

Figure 4. Motor assembly for the middle finger.

Fingerpad Interface. Several interfaces were considered. Strapping the fingerpad to the motor armature was rejected due to possible backlash problems, as well as safety concerns. A thimble design (e.g., Massie & Salisbury, 1994) would probably work well with large-amplitude slow motions, but not with small-amplitude high-frequency vibrations. Our final design simply places the fingerpad on an aluminum pin (diameter: 4.75 *mm*) that is press-fit into each motor's armature (see Fig. 4). This setup has worked very well for the large ranges of amplitudes and frequencies used in this study.

Angular-Position Sensor. The feedback sensor is a precision rotary variable differential transformer (RVDT, Schaevitz, R30A). It was chosen on the basis of its compact size (27 *mm* diameter and 22 *mm* height), high response bandwidth (1 *kHz* nominal), excellent linearity (0.09%, 0.12%, and 0.23% of full-scale displacement for our three factory-calibrated units), and virtually infinite resolution (due to electromagnetic coupling of mechanical input to electrical output). The R30A works with the ATA-101 (Schaevitz), a power-line-operated instrument that provides excitation (10 *kHz*), amplification, and demodulation (rectification and 1 *kHz* lowpass filtering). The three ATA-101s were configured in a master/slave arrangement to synchronize their individual excitation oscillators, thereby minimizing heterodyning interference (i.e., crosstalk) between the three outputs.

Power Amplifier. The Crown D-150A amplifier (Crown International) is a voltage-to-voltage DC-coupled power amplifier with a flat frequency response and near zero phase shift within the frequency range of interest (DC to 300 *Hz*). Although originally designed for driving loudspeakers, it is well suited to drive the head-positioning motors. It can supply 150 *watts* to the motor (which has a typical resistance of 4 *ohms* and negligible inductance of 0.3 *mH*). Unlike pulse-modulated power amplifiers, the Crown D-150A introduces little additional noise or distortion.

Other Supporting Structures. The three motor assemblies are placed on a stool of height 50 *cm*. Foam padding is used between the motor assemblies and the surface of the stool to absorb vibration. The relative positions of the three motor assemblies can be easily adjusted. The motor assemblies are enclosed by a wooden box with an arm support. An opening on the top of the box allows the fingers to reach in and rest on the moving parts of the actuators. For comfort, the box and arm support are covered with foam padding. Finally, felt materials are used between the feet of the stool and the floor to further isolate the entire structure.

Controller Components

Sampling Rate. A sampling rate of 4 *kHz* was used. It was synchronized on all input and output channels. This rate was based on the consideration that (1) the bandwidth of the reference signals was 300 *Hz* and (2) in order to operate within the relatively flat magnitude-response region of a zero-order-hold reconstructive filter, 10 to 20 times oversampling is needed.

DSP Board and I/O Modules. The TMS320C31 board (Spectrum Signal Processing) is a two-thirds length PC/AT format real-time applications platform based around a Texas Instruments 32-bit floating-point digital signal processor. Two Burr-Brown "daughter" modules, each having two input and two output channels (using 16-bit successive approximation converters), are fit onto the board, providing a total of four I/O channels. Three channels are used for normal operation; the fourth channel is used in some performance measurements. All input and output channels include 4th-order Butterworth lowpass filters for anti-aliasing and signal reconstruction, respectively. All the cutoff frequencies are set to 1.55 *kHz* (i.e., < 1/2 sampling rate); their group delays are approximately constant up to 300 *Hz* and average 280 *μsec*.

PID Controller. The controller parameters K_p, K_i, and K_d (for the proportional, integral, and differential terms, respectively) were determined by the Ziegler-Nichols PID stability-limit tuning method (Franklin, Powell, & Workman, 1990). The three motor assemblies have almost identical controllers with average parameters $K_p = 1.95$, $K_i = 118$, and $K_d = 8.1 \times 10^{-3}$. These parameters were implemented digitally (in C code). In order to reduce the noise in the velocity estimates, a 2nd-order digital Butterworth lowpass filter with a cutoff frequency of 300 *Hz* was applied to the (raw) first-order velocity estimate. An anti-windup term was incorporated into the integral term to prevent errors from accumulating. Subsequently, it turned out that the effect of the integral term was negligible in the

sense that the overall system frequency and step responses were hardly affected by the integral term given the parameters summarized above. Therefore, we effectively have a digital PD controller.

PERFORMANCE MEASUREMENTS

Measurements were taken with a dual-channel, real-time spectrum analyzer (Hewlett-Packard 35660A). The default inputs to the spectrum analyzer were the actuator's reference input signal (the intended motion) and the output from the position feedback sensor (the actual motion). The spectrum analyzer measures signals in terms of *dB re 1 V rms (dB V rms)*. A value of 0 *dB V rms* is equivalent to ≈ 76 *dB μm peak*.[2]

Frequency Response

Random noise generated by the spectrum analyzer was sampled with the spare A/D and used as the reference input signal. The actuator's frequency response was measured (essentially) as the ratio of the spectrum of the sampled sensor reading and the spectrum of the reference signal. The command signal sent to the motor was monitored on an oscilloscope to ensure that no "clipping" occurred. Fig. 5 shows the frequency response in terms of magnitude response (above) and group delay (below), measured from 0.5 to 400.5 *Hz* (in 1 *Hz* increments) without the finger contacting the actuator (i.e., "unloaded" condition). Overall, the closed-loop system behaves similar to a 2nd-order lowpass system with a −3 *dB* bandwidth of 50 *Hz* and a roughly 12 dB/octave roll-off at higher frequencies. The resonance frequencies of the three channels are between 28.5 and 30.5 *Hz*, with resonance peaks of 4.1 to 4.5 *dB*. The largest group delay occurs at 32.5 *Hz* (near resonance) and is 14 *msec* for all three channels. At high frequencies, the group delay is 2.5 *msec*; such non-zero delay indicates non-minimum phase behavior.

A second method of checking the response of the closed-loop system involved measuring the system step-response and performing simulations in MATLAB. The step response was measured by recording the sensor signal output with the reference input signal set to a 4 *Hz* square wave. Again, the amplitude was sufficiently small that no saturation of the command signal occurred. The "measured" step response in Fig. 6 (lower panel) shows one half cycle of the normalized recorded sensor signal. The "measured" magnitude gain in Fig. 6 (upper panel) is replotted from the upper panel of Fig. 5. Simulations were performed by computing the frequency-response gain and the step response of a 2nd-order system with no zeros. The "simulated" curves in Fig. 6 show the results obtained with a pair of poles at −65±200*i*. The main features of the frequency and step

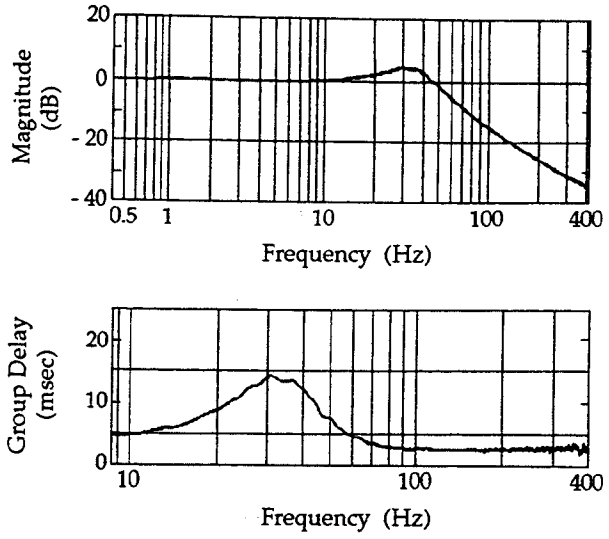

Figure 5. Typical closed-loop frequency response measured with a noise input. Magnitude response, above, and group delay, below.

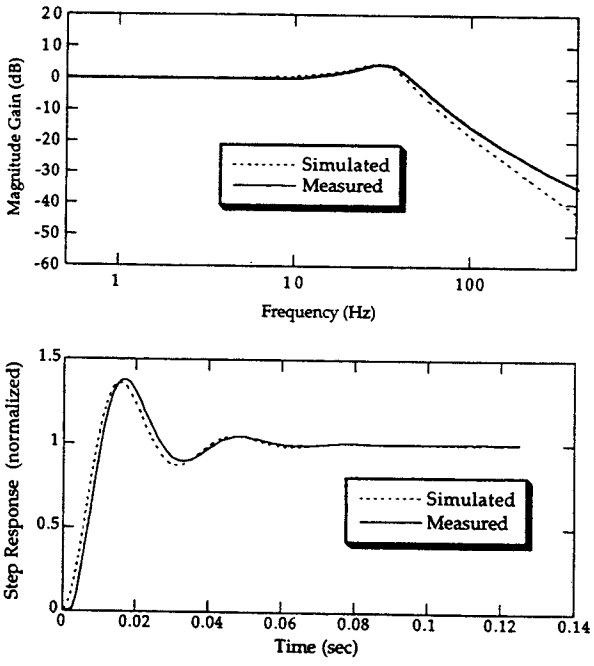

Figure 6. Magnitude gain (above) and step response (below) for measured results and simulations based on a 2nd-order system model.

responses of the closed-loop system are captured by the model. This agreement provides further evidence for the overall linearity of the closed-loop system. The model does, however, underestimate the actuator's high-frequency fall-off. Also, the model, which is

2. For a sinusoidal motion Asin(2πFt), 0 *dB μm peak* is equivalent to $A = 1\ \mu m$, or $A\ rms = 1/\sqrt{2}\ \mu m$. The full range of motion at the contact-point of the moving bar is 25.4 *mm* and it produces a full-scale sensor output of 6 *volts* (peak to peak). Thus 0 *dB μm peak* is equivalent to $\left(10^{-3}/\sqrt{2}\right) \times (6/25.4)\ Vrms = 1.67 \times 10^{-4}\ Vrms$, or approximately −76 *dB V rms*. Equivalently, 0 *dB V rms* is equivalent to ≈ 76 *dB μm peak*.

minimum phase, does not account for the overall delay in the measured step response. This delay is about 10 sampling periods (2.5 *msec*), consistent with that seen above in the group-delay measurements obtained from the noise-input frequency response. Overall, therefore, the closed-loop actuator performance can be characterized approximately as a minimum-phase 2nd-order lowpass system plus an excess delay of 2.5 *msec*.

System Linearity

Sensor signal levels were measured for single-tone inputs with a wide range of reference drive levels. Measurements were taken under both unloaded and "loaded" conditions. For the loaded condition, the index finger rested lightly on the actuator's moving bar (as was found comfortable in other perceptual tests). Fig. 7 shows results at 2, 20, and 200 *Hz* for motion levels ranging from 2 to 56 dB SL; for clarity, the 2-*Hz* results are offset by 20 dB. Also shown are the best-fitting unit-slope straight lines (in the least-square-error sense). All measurements are highly linear as reflected by the high correlation-coefficients (0.996–0.999) for the fitted lines. Loading effects are evident by the reduction in motion for a given drive level. These reductions average 1.5 dB at 2 *Hz*, 2.7 dB at 20 *Hz*, and 0.1 dB at 200 *Hz*. This frequency dependence results from interactions between the actuator's driving point impedance and that from the finger load. Finally, at 200 *Hz*, evidence of motion saturation can be seen for the highest drive level tested (≈ 56 dB SL).

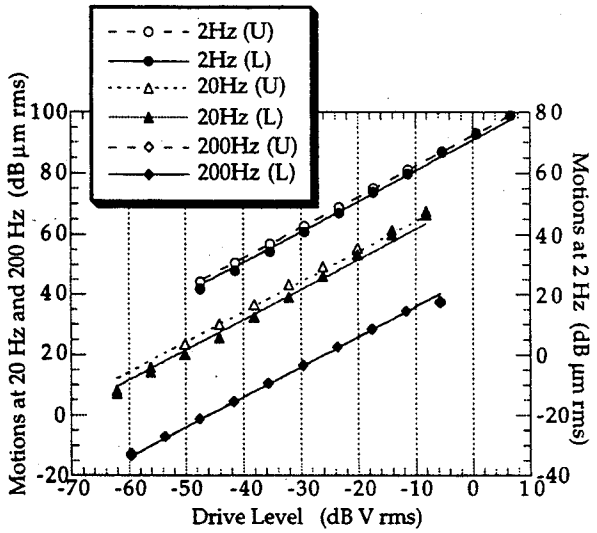

Figure 7. Input-output relationship at three frequency values with best-fitting unit-slope lines. "U" and "L" denote unloaded and loaded conditions, respectively.

Saturation was explored further with measurements taken at 36 and 56 dB SL output levels across a frequency range of 1 to 300 *Hz*. Results indicated that output levels of 36 dB SL can be achieved at any frequency, but 56 dB SL can only be achieved for frequencies up to about 150 *Hz*. At higher frequencies, the maximum signal levels achievable are 55, 53, and 51 dB SL at 200, 250, and 300 *Hz*, respectively. This range is more than adequate for psychophysical studies because stimulation levels exceeding 50–55 dB SL can induce discomfort and fatigue (Verrillo & Gescheider, 1992).

Noise Characteristics

Measurements were taken at the sensor outputs with the reference signals of all three channels set to zero. The sensor output included mechanical noise of the actuator (associated with the closed loop system), the sensor's electrical self-noise, as well as any residual power-line noise. Fig. 8 shows the output from channel 1 which has the highest level of 60-*Hz* power-line noise among the three channels. For comparison, the detection thresholds measured by Bolanowski *et al.* (1988) are also plotted. It can be seen that the most prominent components of the noise spectrum are associated with the power-line frequency of 60 *Hz* and its harmonics at 180 and 300 *Hz*. These components are near or a few dB above the absolute thresholds. The other parts of noise spectrum are low, typically more than 10 dB below threshold.

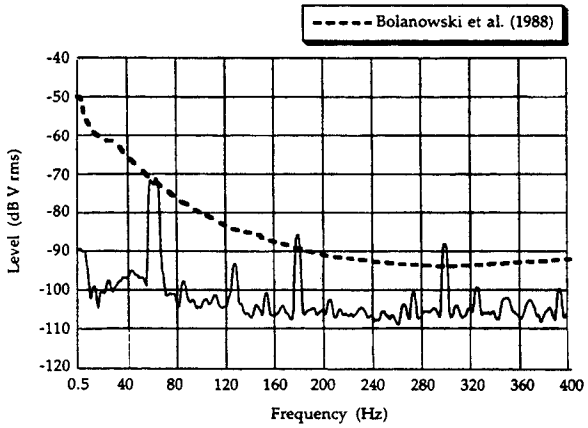

Figure 8. Noise spectrum compared to detection thresholds.

In an attempt to separate the close-loop mechanical noise from electrical noise, the above measurements were repeated with the actuator's moving parts immobilized. The three sensor outputs were essentially the same as that in Fig. 8 except for a 7 dB drop in the level of the 60 *Hz* components. Therefore, most of the measured noise appears to reflect the sensor and its electronics and not motion of the actuator.

Harmonic Distortion

Distortion produced by the actuator system was assessed using single-tone inputs, with frequencies ranging from 1 to 300 *Hz*. The reference drive amplitude was adjusted for each frequency so that the sensor output level (i.e., R30A reading) was roughly 56 dB SL. Using the spectrum analyzer on the sensor output, the levels at the fundamental frequency and at the 2nd up to 6th harmonics were then

recorded. All measurements were performed with loaded and unloaded conditions. The results are presented in Fig. 9 (shown in two panels for clarity). The upper panel shows the results for the 2nd, 3rd and 4th harmonics along with the fundamental output level and the absolute detection threshold — all in *dB V rms* units. The bottom panel shows the results for the 5th and 6th harmonics. Note that the harmonics are plotted at their actual frequencies. For instance, the 2nd, 3rd, 4th, 5th and 6th harmonics of a 100 *Hz* signal are plotted at 200, 300, 400, 500 and 600 *Hz*, respectively. Therefore, the distortion levels can be directly compared with the detection thresholds plotted at the same frequency.

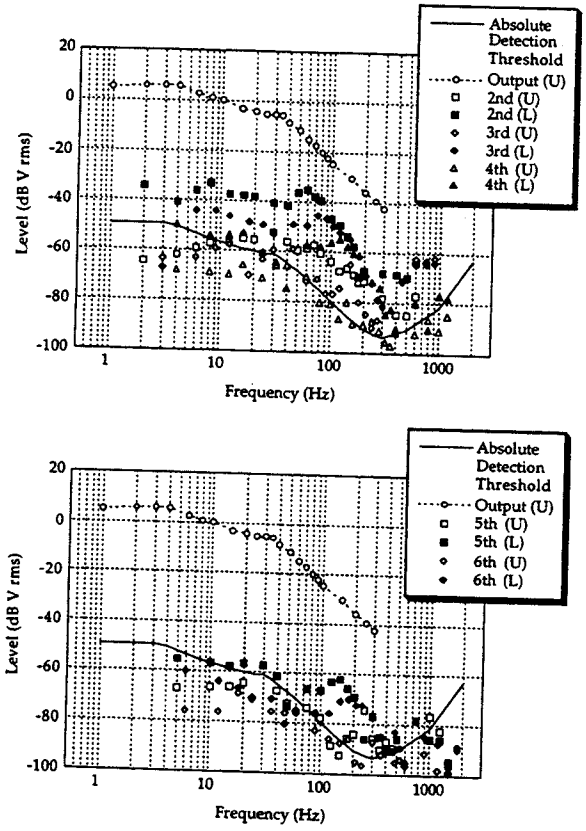

Figure 9. Levels of sensor output signals and harmonics compared with detection thresholds. "U" and "L" denote unloaded and loaded conditions, respectively.

In Fig. 9, the data points for the absolute detection thresholds are taken from Bolanowski *et al.* (1988) for frequencies up to 500 *Hz*, and from Lamore (1984) for frequencies of 1 *kHz* and 2 *kHz*. As expected, the fundamental output levels are above the detection threshold curve by roughly 56 dB, except near 300 *Hz*. In the upper panel, the levels of harmonics 2–4 are at least 40 dB below the fundamental output signal level for the unloaded condition (open symbols). For the loaded condition (filled symbols), however, greater distortion occurs. The maximum distortion occurs with 2nd harmonics near 60 *Hz*. This arises because fundamental frequencies of 30 *Hz* nearly coincide with the system's resonant frequency. The closed-loop gain diminishes near resonance, and finger loading results in asymmetric compression of the sinusoidal stimulus, thereby increasing the 2nd harmonic distortion. However, even in this case the distortion is more than 30 dB below the fundamental output level, and tactual masking may further reduce any effect of this distortion.

The lower panel shows that the 5th and 6th harmonics are at least 60 dB below the fundamental output levels. They are close to, or below, the absolute detection thresholds below 70 *Hz*, and never exceed −60 dB *V rms* (or ≈ 15 dB μm peak).

Similar measurements were repeated using a lower sensor output level of 36 dB SL for selected frequencies (i.e., 1, 3, 10, 30, 100 and 300 *Hz*). Harmonic distortion levels (not shown) are mostly below the corresponding detection thresholds.

Crosstalk

A sinusoid of 2, 20, or 200 *Hz* was used as the reference input for channel 1; both moderate and high levels were tested (35 and 55 dB SL, respectively). The sensor outputs from channels 2 and 3 were measured while their reference inputs were set to zero. The spectral component at the frequency corresponding to that of the reference signal for channel 1 was recorded and expressed in dB relative to motion on channel 1 (see Table 1). At 2 *Hz*, movements on one channel cause very little (immeasurable) crosstalk in the other two channels (< −107 dB); even at an output level of ± 11 *mm* (i.e., 55 dB SL) on channel 1, the crosstalk motion to channels 2 and 3 is below ± 0.05 μm. At 20 *Hz*, crosstalk increases to about −80 dB and at 200 *Hz*, it increases to about −40 dB. Thus, while isolation between channels diminishes as frequency increases, it remains good throughout the operational range.

TABLE 1. Crosstalk measurements. L_1 denotes the level of the test signal on channel 1. L_2 and L_3 denote the levels of the spectral component at the test frequencies on channels 2 and 3, respectively, *relative* to the signal level on channel 1. An asterisk indicates that the level is at the noise floor.

Freq. (*Hz*)	L_1 (dB SL)	L_2 (dB re L_1)	L_3 (dB re L_1)
2	55	−107*	−112*
20	35	−73*	−68*
20	55	−83	−77
200	35	−38*	−43*
200	55	−37	−46

Spectrum of the Sum of Sinusoidal Inputs

One intended use of the TACTUATOR involves the simultaneous presentation of multiple discrete frequency components. Thus, measurements were made to assess the response to such an input. Fig. 10 shows the sensor output spectrum when 2 *Hz*, 30 *Hz* and 300 *Hz* components, at 53, 49 and 47 dB SL, respectively, were applied simultaneously to the reference input. [This is one of the signals used in subsequent psychophysical experiments.] Because of

the spectrum analyzer's limited resolution, the sensor output was measured once with a frequency span of 50 *Hz* (top panel) to view spectral details near the 2 and 30 *Hz* components, and also with a span of 400 *Hz* to show the full spectrum. The upper panel shows that the dominant peaks are at 2 *Hz* and 30 *Hz* (the signal frequencies) at their desired output levels. Harmonics of the 2-*Hz* component (e.g., 4 and 6 *Hz*) as well as intermodulation components at $30 \pm n \cdot 2$ *Hz* ($n = 1, 2, ...$) are also evident; however, all of these distortion components are at least 40 dB below the signal components. The lower panel shows, in addition to the signal-frequency peaks at 2, 30, and 300 *Hz*, distortion components at 60 *Hz* (2×30 *Hz*) and at 330 *Hz* (300+30 *Hz*). Once again, these distortions are small.

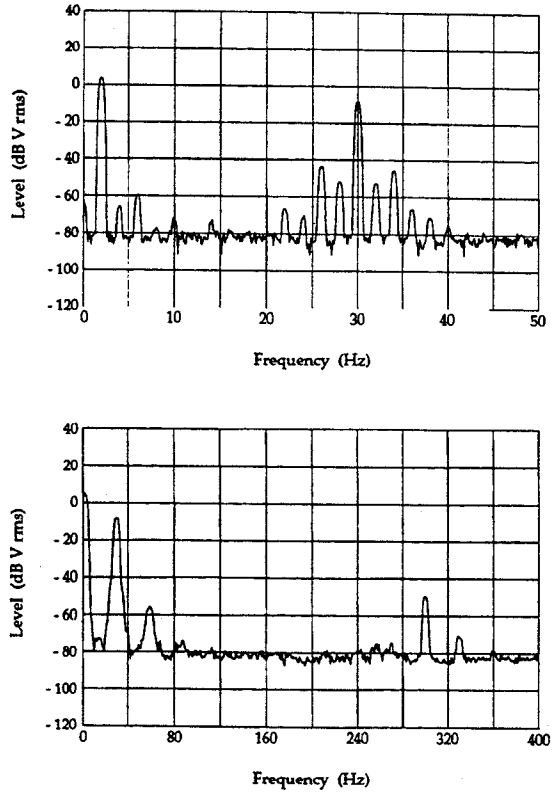

Figure 10. Response to a sum of three sinusoids at 2, 30 and 300 *Hz* measured with an analyzer span of 50 *Hz* (upper panel) and 400 *Hz* (lower panel).

Absolute Detection Thresholds

As a behavioral verification of the TACTUATOR's performance, absolute detection thresholds for sinusoidal stimuli were measured with a one-interval forced-choice paradigm. On each trial, the amplitude of the signal was either zero (i.e., no signal) or A, chosen randomly with equal *a-priori* probabilities. The subject was instructed to report whether the signal was present. For each frequency tested, values of A were chosen to be around the expected threshold. The threshold was estimated as the amplitude corresponding to ≈ 70% correct performance. Results obtained on the index fingers of two subjects (S_1 and S_2) were quite consistent (Fig. 11); they were interpolated to form the absolute detection threshold curve for the TACTUATOR from 2 *Hz* to 300 *Hz* (solid line in Fig. 11). In comparison to reference thresholds from Bolanowski *et al.* (1988), the TACTUATOR thresholds are 9 dB greater for frequencies below 30 *Hz* and equivalent for frequencies above 60 *Hz*. Given the numerous differences between the stimulators used in the two studies (in terms of the fingerpad contactor, the presence of a surround, temperature control, etc.), we consider this agreement good. TACTUATOR thresholds for the other two fingers, the thumb and the middle finger, were also measured for S_1 at selected frequencies; in general, the thresholds for all three digits were similar.

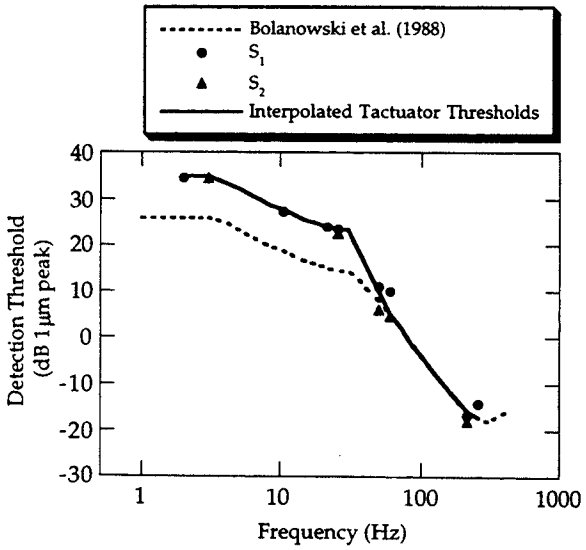

Figure 11. Absolute detection thresholds for the index finger.

The information transmission capabilities with the TACTUATOR have also been assessed through a series of perceptual tests based on identifying discrete sets of stimuli (Tan, 1996). Results are quite promising; estimated information-transfer rate is about 12 *bits/sec*, a rate that is roughly the same as that achieved by Tadoma users in tactual speech communication.

CONCLUDING REMARKS

Taken together, the above measurements indicate that the TACTUATOR serves as a linear positional display throughout its operating range. The useful overall dynamic range of the system exceeds 96 dB. This follows from noting that stimuli of +82 dB *µm* peak can be delivered at low frequencies and threshold stimuli near −14 dB *µm* peak can be delivered near 250 *Hz*. Distortion is generally low. Background noise, including electrical and mechanical components, as well as crosstalk between channels, is also small. Absolute thresholds measured with the TACTUATOR are

in general agreement with those reported in literature. Thus, the TACTUATOR is well suited for a variety of multi-finger tactual perceptual studies.

ACKNOWLEDGMENTS

This research was supported by research grant 2 R01 DC 00126-16 from the National Institute on Deafness and Other Communication Disorders, National Institutes of Health.

REFERENCES

Bolanowski Jr., S. J., Gescheider, G. A., Verrillo, R. T., & Checkosky, C. M. (1988). Four channels mediate the mechanical aspects of touch. *Journal of the Acoustical Society of America*, 84(5), 1680-1694.

Eberhardt, S. P., Bernstein, L. E., Barac-Cikoja, D., Coulter, D. C., & Jordan, J. (1994). Inducing dynamic haptic perception by the hand: system description and some results. *Proceedings of the American Society of Mechanical Engineers*, 55(1), 345-351.

Franklin, G. F., Powell, J. D., & Workman, M. L. (1990). Digital Control of Dynamic Systems (Second Edition ed.). Reading, MA: Addison-Wesley Publishing Company.

Lamore, P. J. J. (1984). Vibrotactile threshold for hairy skin and its transformation into equivalent bone-conduction loss for the mastoid. *Audiology*, 23, 537–551.

Leotta, D. F., Rabinowitz, W. M., Reed, C. M., & Durlach, N. I. (1988). Preliminary results of speech-reception tests obtained with the synthetic Tadoma system. *Journal of Rehabilitation Research and Development*, 25(4), 45-52.

Massie, T. H. & Salisbury, J. K. (1994). The PHANToM haptic interface: A device for probing virtual objects. *Proceedings of the American Society of Mechanical Engineers*, 55(1), 295-299.

Rabinowitz, W. M., Henderson, D. R., Reed, C. M., Delhorne, L. A., & Durlach, N. I. (1990). Continuing evaluation of a synthetic Tadoma system. *Journal of the Acoustical Society of America*, 87(1), 88.

Reed, C. M., Durlach, N. I., Delhorne, L. A., Rabinowitz, W. M., & Grant, K. W. (1989). Special monograph on sensory aids for hearing-impaired persons. *The Volta Review*, 91, 65-78.

Reed, C. M., Rabinowitz, W. M., Durlach, N. I., Braida, L. D., Conway-Fithian, S., & Schultz, M. C. (1985). Research on the Tadoma Method of Speech Communication. *Journal of the Acoustical Society of America*, 77(1), 247-257.

Tan, H. Z. (1996). Information Transmission with a Multi-Finger Tactual Display. Ph.D. Dissertation, Massachusetts Institute of Technology.

Verrillo, R. T., & Gescheider, G. A. (1992). Perception via the sense of touch. In I. R. Summers (Ed.), *Tactile Aids for the Hearing Impaired* (p. 1-36). London: Whurr Publishers.